EBioMedicine 45 (2019) 251–260

Contents lists available at ScienceDirect

EBioMedicine

journal homepage: www.ebiomedicine.com

EBioMedicine
Published by THE LANCET

Regulation of lactate production through p53/β-enolase axis contributes to statin-associated muscle symptoms

Jiajun Huang, Jingjing Du, Wanjun Lin, Ze Long, Na Zhang, Xiaoming Huang, Ying Xie, Liang Liu *, Wenzhe Ma **

State Key Laboratory of Quality Research in Chinese Medicine, Macau University of Science and Technology, Macau, China

ARTICLE INFO

Article history:
Received 1 March 2019
Received in revised form 12 May 2019
Accepted 3 June 2019
Available online 11 June 2019

Keywords:
Statin
Muscle symptoms
Lactate
Dichloroacetate

ABSTRACT

Background: Statin-associated muscle symptoms (SAMS) are the major adverse effects of the class of widely used lipid-lowering agents, and the underlying mechanism remains elusive. In this study, we investigated the potential contribution and molecular mechanism of increased lactate production to SAMS in mice.
Methods: C57BL/6 J mice were administrated with lovastatin and exercise capacity and blood and muscle lactate levels were measured. A variety of metabolic and molecular experiments were carried out on skeletal muscle cell lines A-204 and C2C12 to confirm the *in vivo* findings, and to delineate the molecular pathway regulating lactate production by statins.
Findings: Blood lactate levels of mice treated with lovastatin increased 23% compared to the control group, which was reproduced in type II predominant glycolytic muscles, accompanied with a 23.1% decrease of maximum swim duration time. The *in vitro* evidence revealed that statins increased the expression of muscle specific glycolytic enzyme β-enolase through promoting the degradation of basal p53 proteins, resulting in increased of lactate production. Co-administered with dichloroacetate (DCA), a reagent effective in treating lactic acidosis, reverted the elevated lactate levels and the decreased exercise capacity.
Interpretation: Elevated lactate production by statins through the p53/β-enolase axis contributes to SAMS.
Fund: This work was supported by grants from the Science and Technology Development Fund (FDCT) of Macau (Project codes: 034/2015/A1 and 0013/2019/A1).

1. Introduction

Statins, inhibitors of 3-hydroxy-3-methyl-glutaryl-coenzyme A (HMG-CoA) reductase, are the most widely prescribed drugs worldwide [1]. Millions of people benefit from these lipid-lowering agents to prevent cardiovascular diseases. Although statins are generally well tolerated, patients are suffering from statin-associated muscle symptoms (SAMS), the most common adverse effects of statins. Muscle complaints range from mild myalgia to moderate myopathy and severe rhabdomyolysis with creatine kinase (CK) from normal to marked elevation. The risk of myopathy/rhabdomyolysis is <0.1%, and that of myalgia is up to 25% in observational studies and 1.4% in placebo controlled randomized trials [2]. SAMS causes statin intolerance and lack of adherence, which increases 36% of recurrent myocardial infarction (MI) and 43% of coronary heart disease (CHD) events [3]. The underlying mechanism of SAMS remains elusive, although several hypotheses have been proposed and extensively reviewed. Furthermore, efforts to manage SAMS based on previous findings, like supplementation of vitamin D or coenzyme Q10 (CoQ10), are inconclusive [4,5]. So, new insights into the pathophysiology and treatment of SAMS are warranted.

Lactate is widely accepted as a nociceptive substance. It stimulates afferents during muscle contraction, excites neurons in the locus coeruleus and regulates neuronal plasticity, and enhances the sensitivity of acid-sensing ion channels-3 (ASIC-3), the transducers for nociception and mechanosensation, to low pH [6]. Lactate also increases reactive oxygen species (ROS) production, which could directly interact with and activate the nociceptive system [7]. Increased tissue/blood concentration of lactate has been associated with pain in both physiological and pathological conditions, such as exercise-induced muscle fatigue, incisional pain, discogenic back pain, chronic Achilles tendinopathy, complex regional pain syndrome (CRPS) and chronic inflammatory pain. Importantly, increased interstitial levels of lactate has been found to be a useful biomarker of chronic musculoskeletal pain, which shares similar symptoms with SAMS including muscle weakness, fatigue, aching, stiffness, cramps, and tenderness. Case reports and clinical studies have revealed that statins could cause lactic acidosis or

* Correspondence to: L. Liu, State Key Laboratory of Quality Research in Chinese Medicine, MUST, Building N, Rm. 508, Avenida Wai Long, Taipa, Macau, China.
** Correspondence to: W. Ma, State Key Laboratory of Quality Research in Chinese Medicine, MUST, Building H, Rm. 718e, Avenida Wai Long, Taipa, Macau, China.
E-mail addresses: lliu@must.edu.mo (L. Liu), wzma@must.edu.mo (W. Ma).

https://doi.org/10.1016/j.ebiom.2019.06.003

Research in context

Evidence before this study

Statins are among the most widely prescribed drugs worldwide and are generally well tolerated. However, a substantial number of patients discontinues administration of statins because of statin-associated muscle symptoms (SAMS). Currently, the definition, epidemiology, diagnosis and management of SAMS are conflicting, which could be improved by further understanding of the pathophysiology of the symptoms. Beside previously reported mechanisms, such as sarcolemmal cholesterol reduction, isoprenoid depletion and mitochondrial dysfunction, animal studies and clinical observations have suggested the association of high lactate levels with SAMS.

Added value of this study

In this study, C57BL/6 J mice were administrated with lovastatin and blood lactate levels were found increased compared to the control group. Increased lactate was also present in type II predominant glycolytic muscles rather than type I predominant oxidative muscles, associated with compromised maximum swim duration time. *In vitro* studies on muscle cell lines confirmed the enhancement of lactate production by statins, which was not exclusively a secondary effect of impaired mitochondria. Furthermore, we identified the increased expression of muscle specific glycolytic enzyme β-enolase through promoting the degradation of basal p53 is the underlying mechanism, which was dependent on the inhibitory activity on HMG-CoA reductase of statins. Based on these observations, when dichloroacetate (DCA), a reagent effective in treating lactic acidosis, was co-administered, statin-induced lactate elevation and compromised exercise capacity were reverted in mice.

Implications of all the available evidence

These data suggest that the increase of lactate production by statins through p53/β-enolase axis may contribute to SAMS. Co-administration of DCA is a potential avenue to alleviate the symptoms.

increased blood lactate/pyruvate ratio or respiratory exchange ratio (RER) [8–11]. Similar results have also been demonstrated in animal studies [12–15]. However, other studies found no obvious elevation of lactate levels with statins treatment [16,17]. This evidence promotes us to investigate whether statins affect lactate levels and their role in SAMS in mice.

In this study, we demonstrate that increased lactate production is associated with SAMS as manifested by reduced maximum exercise capacity of mice treated with statins. We further report that statins can directly increase lactate production by alleviating the negative regulation of glycolysis by p53, which transcriptionally represses *ENO3* gene that encoding muscle specific β-enolase. Co-administration with dichloroacetate (DCA), an agent effective in lactic acidosis management, promotes lactate recovery and improves statin-induced decrease of exercise capacity. Thus, our study provides a new vision of SAMS.

2. Materials and methods

2.1. Cell culture and reagents

The human rhabdomyosarcoma cell line A-204 and the mouse myoblast C2C12 cell line were obtained from ATCC, and maintained in McCoy's 5A medium (Gibco) and Dulbecco's modified Eagle's medium (Gibco) respectively. C2C12 myoblasts were stimulated to differentiate into myotubes by switching to the medium with 2% horse serum. The human colon cancer HCT116 *SCO2*−/− cell line was a generous gift from Dr. Paul M. Hwang at the National Institutes of Health, and cultured in McCoy's 5A medium.

Lovastatin, fluvastatin sodium, simvastatin, rosuvastatin calcium, mevalonic acid sodium, sodium dichloroacetate, coenzyme Q10 (CoQ10) and oligomycin A were purchased from Sigma Aldrich. Pitavastatin and atorvastatin were purchased from Cayman Chemical. Nutlin-3 was purchased from Selleck Chemicals. The doses of statins in cell culture were consistent with previous studies in SAMS [18].

2.2. Animal studies

All mice were handled and maintained in accordance with the Animal Care and Use Committee of Macau University of Science and Technology. C57BL/6 J female mice were obtained from the Chinese University of Hong Kong and were administrated with lovastatin (50 mg/kg/2 days) alone, similar dose as previous studies in SAMS [15,19], or together with dichloroacetate (DCA, 40 mg/kg/day) by gavage at 8 weeks old. Maxim swimming capacity was measured as previously reported [20]. Briefly, the mice were acclimated to swimming for 5 min/day for 3 days before the formal swimming test. The mice were loaded with a 2 g iron block attached to the tail and the swimming durations to exhaustion were measured in a temperature-controlled (34 °C) tank. The blood lactate concentrations of mice at rest were analyzed using a hand-held lactate analyzer Lactate Scout+ (EKF Diagnostics).

2.3. Glucose, lactate and ATP concentrations assessment

Cells with indicated treatments were changed with fresh medium and incubated for an additional 8 h. Culture medium was collected, and glucose and lactate concentrations were determined using the Glucose (GO) Assay Kit (Life technology) and the Lactate Assay Kit (Trinity Biotech) respectively. Intracellular lactate was detected by HPLC (1290 series, Agilent Technologies) coupled with triple TOF 6600 (Q-TOF, AB Sciex). Intracellular ATP level was determined by ATP Determination Kit (Molecular Probes) according to the manufacturer's protocol.

2.4. Glucose uptake assay

Cells were seeded in 6-well plates and incubated with fluvastatin for 48 h. The cells were washed three times by PBS and resuspended in 500 μl PBS containing 100 μM 2-N-7-(nitrobenz-2-oxa-1,3-diazol-4-yl) amino-2-deoxy-D-glucose (2-NBDG, Invitrogen). After 20 min incubation at 37 °C in dark, cells were washed three times with ice-cold PBS and analyzed on flow cytometer (Becton Dickinson).

2.5. Extracellular flux assay

To evaluate the bioenergetic function of skeletal muscle cells in response to statins, we performed extracellular flux assays using XFp Extracellular Flux Analyzer (Seahorse Bioscience). Cells with indicated treatments were seeded in XFp cell culture miniplates. After incubation overnight, cells were washed with and changed to XF assay medium and incubate at 37 °C in a non-CO_2 incubator for 1 h. Baseline extracellular acidification rate (ECAR) and oxygen consumption rate (OCR) were recorded 6 times with an interval of 6 min. Maximum ECAR was read after administration of oligomycin (10 μM).

2.6. Western blotting

Proteins were extracted using ice-cold RIPA buffer supplemented with protease inhibitor cocktail (Roche), separated by 4% - 20% SDS PAGE, transferred to PVDF membrane (Millipore), and visualized by

the SuperSignal West Pico Chemiluminescent Substrate (Thermo Fisher Scientific). Antibodies against p53, β-enolase, HIF 1-α, c-Myc, TIGAR and Glut2 were obtained from Santa Cruz Biotechnology. Antibodies against MDM2, phospho-MDM2 (S166) and Glut1 were obtained from Abcam. Antibodies against Aldolase A, phospho-Akt, HK1, PKM1/2 and LDHA were obtained from Cell Signaling Technology. Antibody against β-actin was obtained from Sigma.

2.7. Immunoprecipitation

Cells with indicated treatment were washed with PBS and harvested using ice-cold cell lysis buffer (150 mM NaCl, 50 mM Tris-HCl pH 8.0, 1% NP-40) containing protease and phosphatase inhibitors. Cell lysate was then centrifuged and the supernatant was collected. To capture the immune complexes, Protein A/G PLUS-Agarose (Santa cruz) bead slurry (preclear and pre-equilibrated in the cell lysis buffer) was added into the cell lysate and incubated overnight at 4 °C on a rotator. The beads were washed by ice-cold cell lysis buffer and 1× SDS-PAGE sample loading buffer was added. Centrifuged and collected the supernatant carefully. The immunoprecipitate (supernatant) was load onto an SDS-PAGE gel for western blotting analysis.

2.8. Identification of p53 repressive response elements and chromatin immunoprecipitation (ChIP) assay

We used UCSC Genome Browser (http://genome.ucsc.edu/) to obtain the human *ENO3* genomic sequence. The potential p53 repressive response elements (p53RREs), which are consisting of four canonical p53-binding sites (5'-RRRCW-3′) arranged head to tail and matching >90%, were identified by Vector NTI Advance 10 software (Invitrogen).

ChIP assay was performed with ChIP-IT Express (Active Motif) following the manufacturer's protocol. A-204 cells were fixed with 1% formaldehyde on a shaking platform for 10 min at room temperature following by sonication to shear the chromatin. Samples were immunoprecipitated with mouse monoclonal anti-p53 antibody or control mouse IgG serum (10 μg/ml) for PCR amplification. *CD44* served as the positive p53RRE control [21].

Sequences of RT-PCR primer pairs for the putative p53RREs:

ENO3-RRE1 (Foward:5′-CAGGCAATGTCTGGATCACCG-3′, Reverse:5′-CTGACTGCGAAGAAACCCAAAG-3′)

ENO3-RRE2 (Foward:5′-CCTGTCTAAATTCGTTTCCTGTCC-3′, Reverse:5′-CACCCCAGGATTACATTCCC-3′)

ENO3-RRE3 (Foward:5′-TTGACCTTTGGTAAGGGGGC-3′, Reverse:5′-AGCCAATACCATGCTCACCC-3′)

CD44-RRE (Foward:5′-TTTACGGTTCGGTCATCCTC-3′, Reverse:5′-TGCTCTGCTGAGGCTGTAAA-3′)

2.9. Promoter reporter assay

Oligonucleotides containing the putative *ENO3* p53RRE3 or the mutated p53RRE3 sequences were annealed and cloned into the pNL3.2 [NlucP/minP] nanoluciferase vector (Promega) between *Sac*I and *Xho*I restriction sites. ENO3-p53RRE3-WT-F:5′-CGGGGTGAGCTGACACTGTCCCAGCTGCCACCTAGACTCGGAGCTCCATC-3′, ENO3-p53RRE3-WT-R:5′-TCGAGGATGGAGCTCCGAGTCTAGGTGGCAGCTGGGACAGTGTCAGCTCACCCCGAGCT-3′, ENO3-p53RRE3-MUT-F:5′-CGGGGTGAGCTGACACTGTCCCAGCTGCCACCTAGATCCGGACCTCCATCC-3′, ENO3-p53RRE3-MUT-R:5′-TCGAGGATGGAGGTCCGGATCTAGGTGGCAGCTGGGACAGTGTCAGCTCACCCCGAGCT-3′.

A-204 cells were co-transfected with the reporter plasmids and the transfection efficiency control plasmid (pGL4.54 [luc2/TK]) containing TK promoter and firefly luciferase. The luminescence activities of the firefly luciferase and the nanoluciferase were sequentially measured with the Nano-Glo® Dual-Luciferase® Reporter Assay System following the manufacturer's instruction (Promega).

2.10. Lentivirus mediated mRNA knockdown and cDNA expression

Oligonucleotides containing the p53 and HMGCR shRNA sequences were cloned into the pLKO.1 plasmid (Addgene, 10,878) and verified by sequencing. Plasmid containing the non-specific shRNA (SHC002, Sigma) was used as a negative control for gene knockdown.

shp53-1:5′-CCGGCGGCGCACAGAGGAAGAGAATCTCGAGATTCTCTTCCTCTGTGCGCCGTTTTTG-3′, shp53-2:5′-CCGGGTCCAGATGAAGCTCCCAGAACTCGAGTTCTGGGAGCTTCATCTGGACTTTTTG-3′, shHMGCR-1:5′-CCGGCTATGATTGAGGTCAACATTACTCGAGTAATGTTGACCTCAATCATAGTTTTTG-3′, shHMGCR-2:5′-CCGGGGTTCTAAAGGACTAACATAACTCGAGTTATGTTAGTCCTTTAGAACCTTTTTG-3′.

The empty plasmid pLenti-CMV and the plasmid containing *ENO3* cDNA (accession number NM_001976) were obtained from Public Protein/Plasmid Library. Lentiviruses were generated by co-transfected of lentiviral plasmids and the MISSION packing mix (Sigma) into HEK293T cells according to the manufacturer's protocol. A-204 cells were transduced with lentivirus for mRNA knockdown or cDNA expression and selected with puromycin before further analysis.

2.11. Real-time PCR quantitation

Cellular mRNA was extracted using the Dynabeads mRNA Direct Kit (Life Technologies) and cDNA was synthesized by the SuperScript III reverse transcriptase (Life Technologies) according to the manufacturer's instructions. Quantitative real-time PCR analysis was performed on the ViiA™ 7 Real-Time PCR System (Applied Biosystems). Cellular mRNA expression levels of target genes were normalized to the eukaryotic translation initiation factor (EIF3S5).

2.12. Statistical analyses

Data are shown as the mean ± SD unless otherwise stated. Statistical analyses between two groups were performed by two-tailed distribution Student's *t*-test using Microsoft Excel. When more than two groups were compared, data were analyzed by one-way ANOVA using GraphPad Prism 5 software. When a significant F ratio was confirmed,

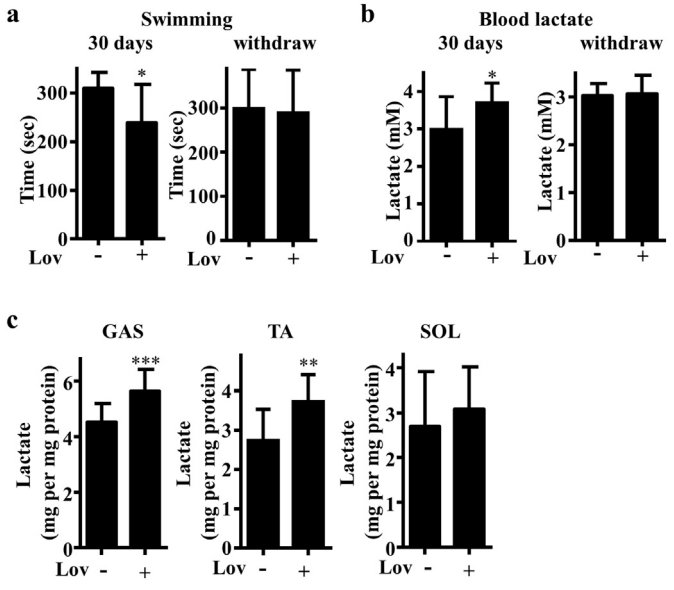

Fig. 1. Lovastatin attenuates exercise capacity in mice and increases blood and muscle lactate levels. (a) Maximum swimming duration times of C57BL/6 J mice administered with lovastatin for 30 days and after the drug withdrawn for an additional 14 days (n = 10 each group). (b) Resting blood lactate levels before the swimming test (n = 10 each group). (c) Lactate concentrations in gastrocnemius (GAS), tibialis anterior (TA) and soleus (SOL) muscles of mice administered with lovastatin for 30 days (n = 10 each group). Data are shown as mean ± SD,$^{*}P < .05$, $^{**}P < .01$, $^{***}P < .001$ (Student's *t*-test).

the difference was further analyzed by Tukey's test. Significant differences were indicated as *($P < .05$), **($P < .01$) or ***($P < .001$) according to the level of significance.

3. Results

3.1. Lovastatin attenuates exercise capacity in mice and increases blood and muscle lactate levels

Decreased exercise capacity has been reported as the behavioral feature in animal models of SAMS [15,22,23]. To validate the mouse model in this study, we performed swimming endurance test in mice treated with lovastatin. As expected, the maximum swim times were significantly reduced by 23.1% ± 8.6% ($P = .016$, Student's *t*-test) in mice treated with lovastatin for 30 days comparing to the control group (Fig. 1a). The loss of exercise capacity returned to normal 2 weeks after drug withdraw (Fig. 1a), which is complied with the clinical diagnostic criteria of SAMS [24]. Blood lactate was increased by 23% ± 10.5% ($P = .045$, Student's *t*-test) at 30 days under resting conditions with lovastatin treatment (Fig. 1b). The increased blood lactate levels persisted as long as the treatment continues up to 30 weeks (Supplemental Fig. 1a). In accordance with recovered exercise capacity, stopping

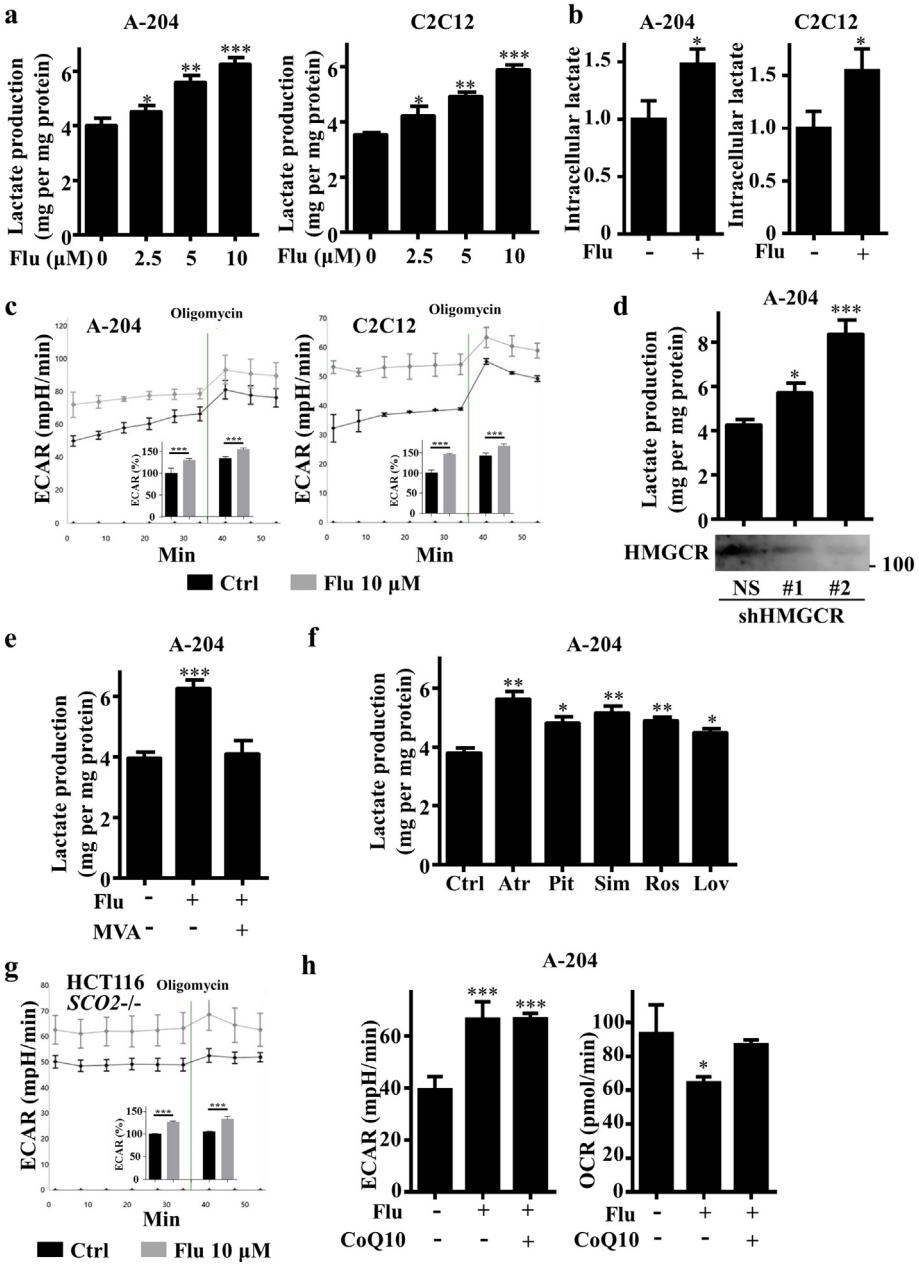

Fig. 2. Statins increase lactate production in cultured skeletal muscle cell lines. (a) Dose-response of fluvastatin treatment for 48 h on lactate production in A-204 cells and C2C12 myotubes ($n = 3$). (b) Effect of fluvastatin (10 μM) treatment for 48 h on intracellular lactate levels normalized to the untreated control cells (n = 3). (c) Baseline and maximum (stimulated by oligomycin) extracellular acidification rate (ECAR) after fluvastatin (10 μM) treatment for 48 h (n = 3). Insert is the average normalized to control in baseline. (d) Lactate production after lentivirus-mediated knockdown of HMGCR in A-204 cells cultured for 48 h (n = 3). HMGCR protein assessed by western blotting. (e) Effect of mevalonate (MVA, 200 μM) on fluvastatin-induced (10 μM) lactate production in A-204 cells ($n = 3$). (f) Lactate production in A-204 cells exposed to atorvastatin (Atr), pitavastatin (Pit), simvastatin (Sim), rosuvastatin (Ros), and lovastatin (Lov) at 10 μM for 48 h ($n = 3$). (g) Baseline and maximum (stimulated by oligomycin) extracellular acidification rate (ECAR) in HCT116 *SCO2*−/− cells with fluvastatin (10 μM) treatment for 48 h (n = 3). Insert is the average normalized to control in baseline. (h) Effect of Coenzyme Q10 (1 μM) on baseline extracellular acidification rate (ECAR) and oxygen consumption rate (OCR) following fluvastatin (10 μM) treatment for 48 h (n = 3). Seahorse XF Analyzer assay data are shown as mean ± SEM, other data are shown as mean ± SD, *$P < .05$, **$P < .01$, ***$P < .001$ (Student's *t*-test).

administration of lovastatin decreased blood lactate levels back to normal (Fig. 1b).

As skeletal muscles are the lesion sites affected by SAMS and also the major tissues producing lactate, we measured the effect of lovastatin on lactate concentrations in different muscles. We found that lactate levels were significantly higher in type II predominant glycolytic muscles gastrocnemius (GAS) and tibialis anterior (TA) (Fig. 1c). There was a trend, although not significant, of increased lactate in the other two glycolytic muscles extensor digitorum longus (EDL) plantaris (PLA) (Supplemental Fig. 1c), suggesting that statins may enhance glycolysis resulting in increased lactate production. In line with this idea, there was no significant change in soleus (SOL), which is type I predominant oxidative muscle (Fig. 1c).

There was no elevation of plasma CK levels in mice treated with lovastatin (Supplemental Fig. 1b), indicating no severe rhabdomyolysis was induced in this study. This was further confirmed by histological

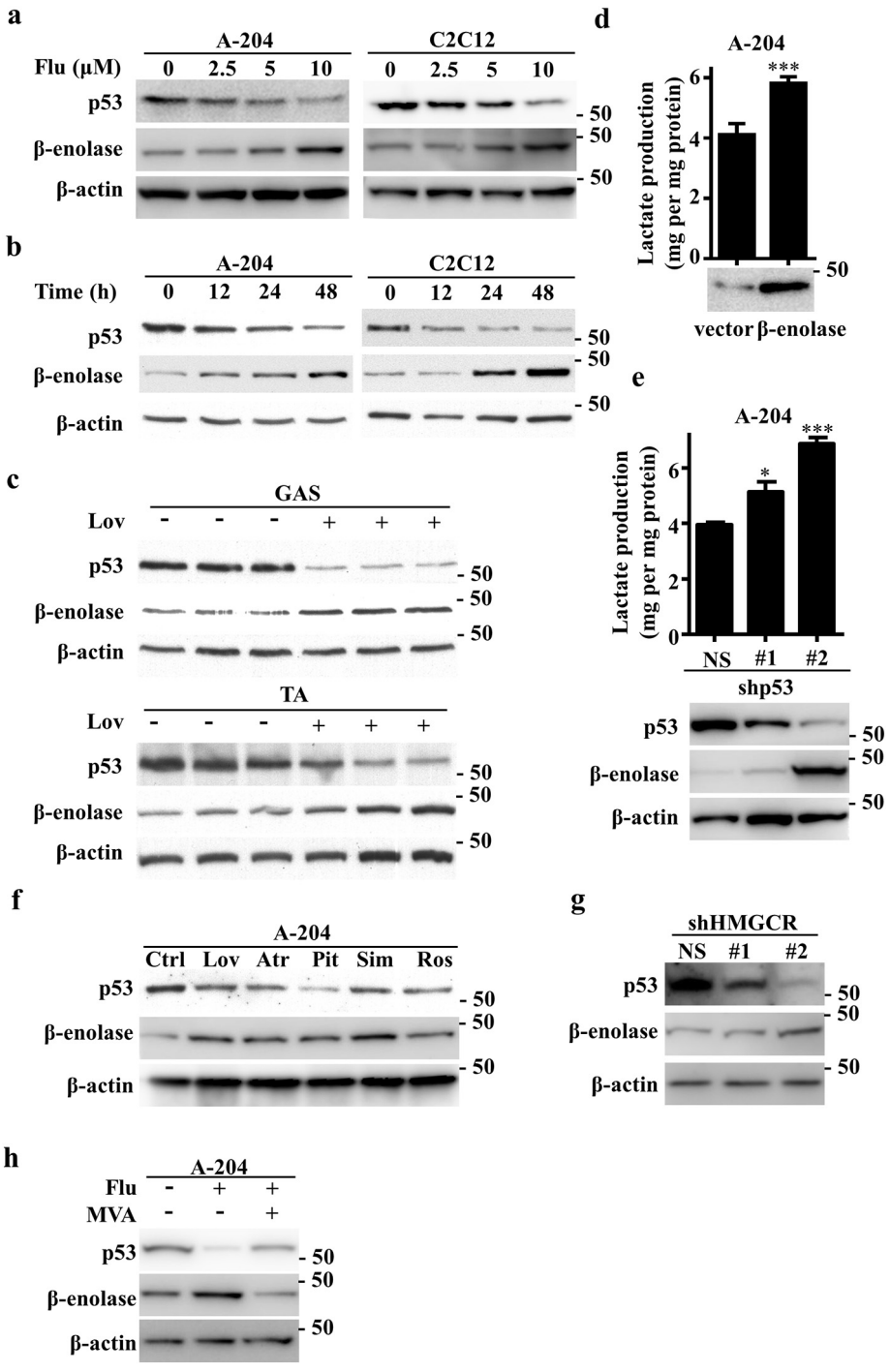

Fig. 3. p53/β-enolase axis mediates statin-induced lactate production (a) Dose effect (48 h) and (b) time-course (10 μM) of fluvastatin on the protein levels of p53 and β-enolase in A-204 cells and C2C12 myotubes. (c) p53 and β-enolase protein levels in gastrocnemius (GAS) and tibialis anterior (TA) muscles of mice treated with lovastatin for 30 days. (d) Lactate production in A-204 cells exogenously expression of β-enolase ($n = 3$). (e) Lactate production after lentivirus-mediated knockdown of p53 in A-204 cells (n = 3). p53 and β-enolase protein assessed by western blotting. (f) p53 and β-enolase protein in A-204 cells exposed to atorvastatin (Atr), pitavastatin (Pit), simvastatin (Sim), rosuvastatin (Ros), and lovastatin (Lov) at 10 μM for 48 h. (g) p53 and β-enolase protein in A-204 cells after lentivirus-mediated knockdown of HMGCR. (h) Effect of mevalonate (MVA, 200 μM) on the protein level of p53 and β-enolase following fluvastatin (10 μM) treatment for 48 h. Data are shown as mean ± SD, $^{*}P < .05$, $^{***}P < .001$ (Student's t-test).

analysis with GAS and TA muscles showing no obvious morphologic changes (Supplemental Fig. 1d). This discrepancy between functional changes and morphological changes in statin treated mice was also reported previously [19]. Furthermore, lovastatin treatment neither changed the body weight significantly nor caused any obvious physical/health problems of the mice. Taken together, these results imply that increased lactate levels are associated with SAMS, especially mild myalgia.

3.2. Statins increase lactate production in cultured skeletal muscle cell lines

To verify the observed increased lactate levels in mice with lovastatin treatment, we measured lactate production in mouse C2C12 myotubes and human A-204 rhabdomyosarcoma cell lines, both were widely used in muscle biology studies. As shown in Fig. 2a, fluvastatin augmented lactate released into the culture medium 12%–56% in A204 cells and 19%–67% in C2C12 myotubes respectively at the indicated concentrations. This was further confirmed by the elevated intracellular levels of lactate (Fig. 2b), as well as by the increased extracellular acidification rate (ECAR) at both baseline and maximum level stimulated by mitochondrial ATP synthase inhibitor oligomycin (Fig. 2C). Increased lactate production was in accordance with increased glucose consumption as evidenced by direct measurement of residue glucose in the medium (Supplemental Fig. 2a) and by flow cytometric analysis of the fluorescent deoxyglucose analog 2-NBDG (Supplemental Fig. 2b).

Statins inhibit the rate-limiting enzyme, HMG-CoA reductase (HMGCR), in the cholesterol synthesis pathway. To confirm the specificity of the elevated lactate production with the inhibition of HMGCR by statins, we carried out lentivirus-mediated knockdown of the enzyme and found increased lactate productions by two distinct lentiviral hairpins (Fig. 2d). Supplementation of mevalonic acid (MVA), the immediate product of HMGCR, restored statin-induced lactate levels (Fig. 2e and Supplemental Fig. 2c). Furthermore, other statins currently used in the clinic also increased lactate production in A-204 cells (Fig. 2f) and in C2C12 myotubes (Supplemental Fig. 2d).

Statins affect mitochondrion functions through multiple mechanisms, as extensively reviewed [25]. Indeed, fluvastatin inhibited oxygen consumption rate (OCR) and decreased intracellular ATP levels in muscle cells (Supplemental Fig. 2f and Supplemental Fig. 2e). The question of the observed increased lactate production is whether it is the direct effect of statins or the metabolic compensatory effect of impaired mitochondria. After administration of oligomycin, the compound inhibiting respiration, increased ECAR (Fig. 2c) with fluvastatin treatment persisted. To further clarify this question, we took advantage of the human colon cancer cell line HCT116 depleted of *SCO2* gene, which is deficient of mitochondrial respiration [26]. As expected, treatment with fluvastatin had no effect on the OCR of the cells (Supplemental Fig. 2 g). However, fluvastatin still increased lactate production in HCT116 *SCO2*−/− cells despite the non-functional mitochondria (Fig. 2g). CoQ10 rescued the oxidative metabolism in muscle cells treated with fluvastatin (Fig. 2h), which is consistent with the previous

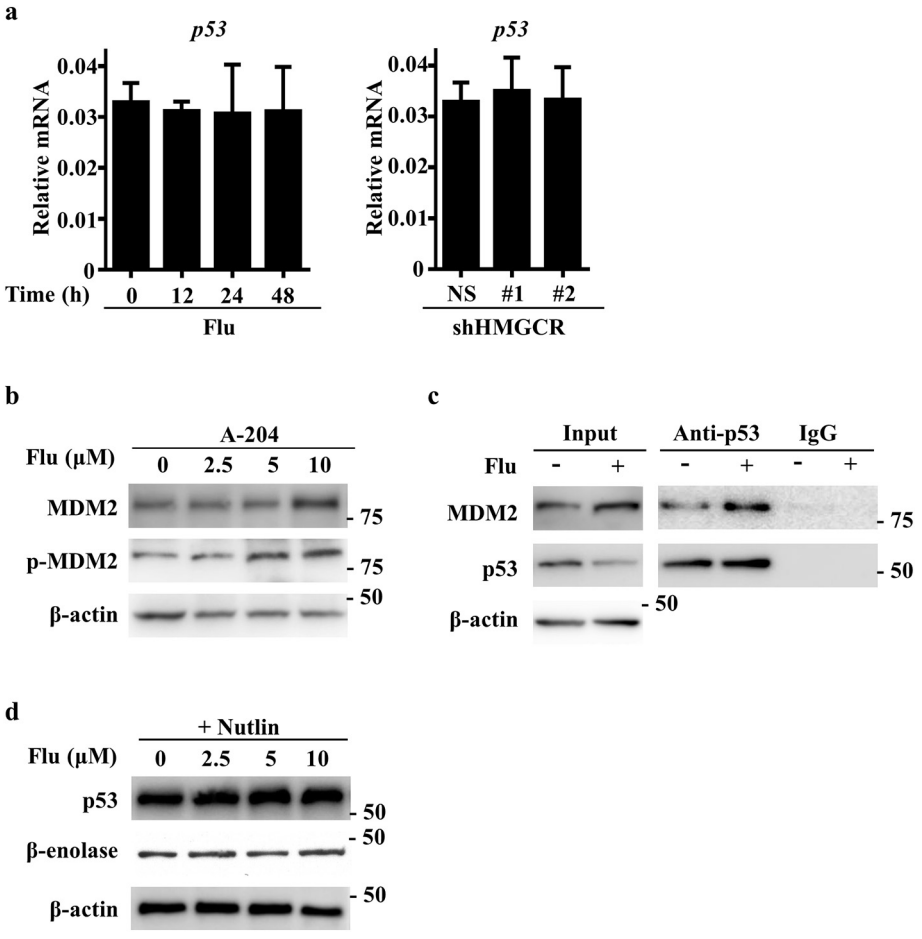

Fig. 4. Fluvastatin promotes p53 degradation *via* enhanced MDM2 phosphorylation. (a) *p53* mRNA levels with fluvastatin (10 μM) treatment at the indicated time (left panel) and after HMGCR knocking down (right panel) in A-204 cells (n = 3). (b) Total and phosphorylated MDM2 (Ser166) protein levels with fluvastatin (10 μM) treatment in A-204 cells for 48 h. (c) Cytosolic extract of A-204 cells treated with fluvastatin (10 μM) for 48 h were immunoprecipitated (IP) with control IgG or anti-p53 antibody. MDM2 and p53 proteins assessed by western blotting. (d) p53 and β-enolase protein in A-204 cells exposed to Nutlin-3 (10 μM) and fluvastatin at indicated concentrations for 48 h. Data are shown as mean ± SD.

studies [18]. However, the ECAR remained the same as fluvastatin treated regardless of CoQ10 supplementation (Fig. 2h). Our findings indicate that the enhanced lactate production cannot be attributed exclusively as a secondary effect of impaired mitochondria.

3.3. p53/β-enolase axis mediates statin-induced lactate production

Lactate is the end product of anaerobic glycolysis. In order to find out the underlying mechanism of increased lactate production with statins treatment, we checked the expression levels of enzymes in the glycolysis pathway as well as the known upstream regulators. We did not observe significant changes in glycolysis enzymes, like hexokinase-1 (HK1), aldolase A, pyruvate kinase isozymes M1/M2 (PKM1/M2) and lactate dehydrogenase A (LDHA) (Supplemental Fig. 3). But it was interesting that β-enolase increased with fluvastatin treatment both dose- and time-dependently (Fig. 3a and 3b). β-enolase is the muscle-specific isoform of enolases, converting 2-phosphoglycerate to phosphoenolpyruvate in the glycolysis pathway, and is expressed higher in type II muscle fibers than type I fibers [27]. Consistent with being the muscles with significantly increased lactate (Fig. 1c), glycolytic type II fibers GAS and TA exhibited higher β-enolase proteins following lovastatin treatment (Fig. 3c). Exogenous expression of β-enolase significantly increased lactate production in A-204 cells (Fig. 3d).

We then checked protein levels of well-characterized upstream regulators of glycolysis including hypoxia-inducible factor 1- α (HIF 1-α), c-Myc, phospho-Akt and TP53-inducible glycolysis and apoptosis regulator (TIGAR), and there were no significant changes of these proteins (Supplemental Fig. 3). The lack of consistency of induced phospho-Akt by stains with previous publication probably dues to different experiment systems [28]. However, tumor suppressor p53, which has been found regulating glycolysis through multiple pathways in last decade [29], was significantly decreased by statins in both muscle cells (Fig. 3a and 3b) and tissues (Fig. 3c). Our finding implies the possible regulation of β-enolase by p53 following statin treatment. To verify this observation, p53 was knocked down by lentivirus-mediated shRNA in A-204 cells and we found that reduced expression of p53 proteins caused the increment of β-enolase and lactate production (Fig. 3e). The correlation of p53 and β-enolase was reproduced with other statins (Fig. 3f). The specificity of the regulation of p53/β-enolase axis by the inhibition of HMGCR with statins was confirmed by both HMGCR knockdown (Fig. 3g) and MVA supplementation experiments (Fig. 3h) in A-204 cells.

To understand the underlying mechanisms of statin-induced p53 down-regulation, we first measured the mRNA levels of p53 in A-204 cells. There were no obvious changes neither with fluvastatin treatment nor with HMGCR knockdown (Fig. 4a), indicating that statins may affect

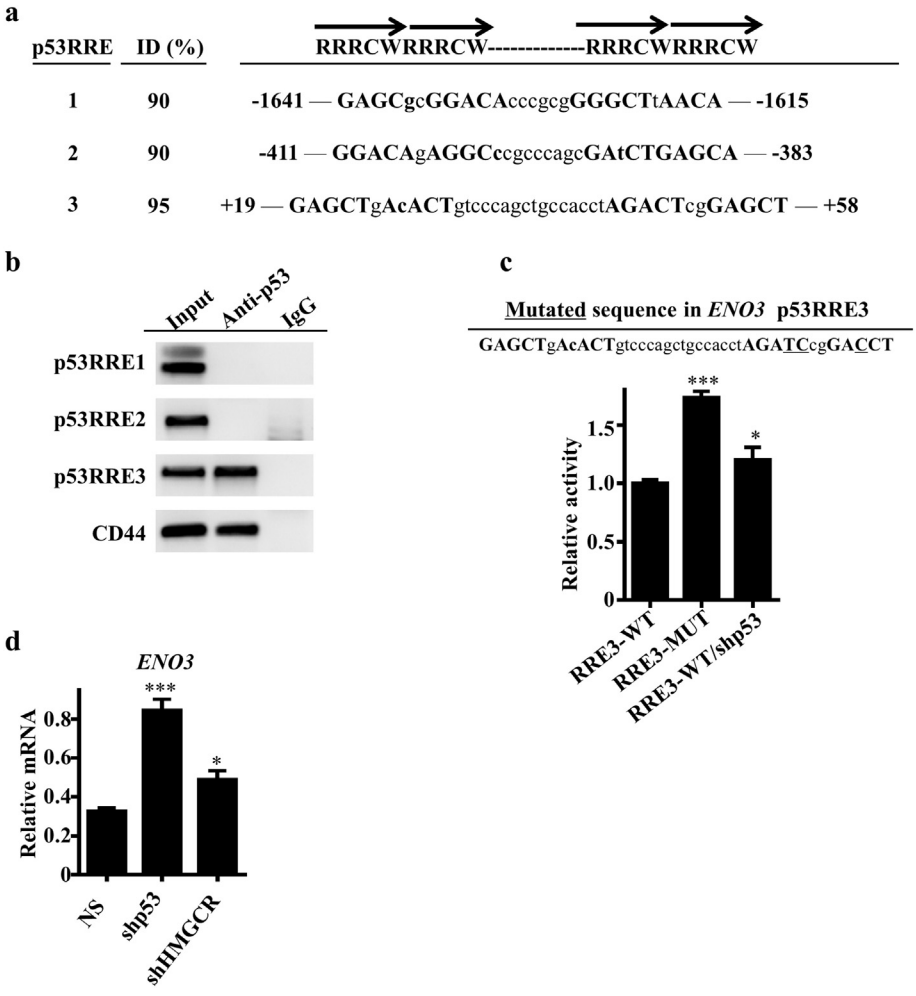

Fig. 5. p53 transcriptional represses *ENO3*. (a) The putative p53 repressive response elements (p53RREs) in human *ENO3* promoter, relative to bp +1 position of the transcription start site (TSS), are shown in bold. The matching consensus p53RRE bases are shown in uppercase characters. ID% indicates the identity. R, purine; W, A, or T base. (b) Chromatin immunoprecipitation (ChIP) assay to present the interaction between *ENO3* p53RREs and p53 protein in A-204 cells. Chromatin from A-204 cells was immunoprecipitated (IP) with either anti-p53 antibody or control IgG. The obtained DNA fragments were amplified by PCR using a set of primer pairs surrounding the p53RRE sites in the *ENO3* promoter. The p53RRE of *CD44* gene was used as a positive control. (c) The point mutations introduced into p53RRE3 are shown in underscore characters. Luciferase reporter assay of wild type (RRE3-WT), mutated (RRE3-MUT) and knockdown of p53 (RRE3-WT/shp53) of *ENO3* p53RRE3 in A-204 cells ($n = 3$). (d) *ENO3* mRNA level in response to p53 and HMGCR knocking down in A-204 cells (n = 3). Data are shown as mean ± SD, $^{*}P < .05$, $^{***}P < .001$ (Student's *t*-test).

p53 protein stability. Statins have been reported to increase phosphorylation of MDM2 at Ser166, which can promote p53 degradation [30]. Indeed, fluvastatin increased MDM2 phosphorylation dose-dependently (Fig. 4b) and enhanced the binding of MDM2 with p53 proteins (Fig. 4c). Inhibition of MDM2-p53 interaction by nutlin nullified the effect of fluvastatin on the protein levels of p53 and β-enolase (Fig. 4d).

These data suggest that statins regulate lactate productions through the p53/β-enolase axis.

3.4. p53 transcriptional represses ENO3

The next crucial question to address is how the loss of basal p53 by statins down regulates β-enolase. As a transcription factor, p53 represses gene expression through binding to the DNA motif consisting of four canonical p53-binding sites arranged head to tail (p53RRE) [21,31]. We scanned the *ENO3* promoter (−2000 to +100) and found 3 putative p53RRE sites with >90% identity (Fig. 5a). We first carried out chromatin immunoprecipitation (ChIP) in A-204 cells to test whether p53 can bind to these putative p53RRE sites. Only p53RRE3, the one with highest homology (95% identity) to the p53 repressive consensus sequence, was pulled down by the anti-p53 antibody comparing with nonspecific control IgG (Fig. 5b). A specific p53 repressive binding site in the *CD44* gene served as the positive control. The repressive effect of basal p53 on p53RRE3 was tested by promoter reporter assay. As shown in Fig. 5c, the luciferase reporter construct containing three point mutations in p53RRE3 (RRE3-MUT) displayed significant higher activity than the wild type construct (RRE3-WT). In addition, knockdown of endogenous p53 increased the luciferase signal (Fig. 5c). Finally, the mRNA levels of *ENO3* were significantly elevated when knocking down of either *p53* or *HMGCR*, further verified the transcriptional repressive activity of baseline levels of p53 on *ENO3* and the suggested signal axis of statins on lactate production (Fig. 5d).

3.5. Dichloroacetate decreases lactate accumulation and improves decline in exercise capacity in mice treated with lovastatin

Dichloroacetate (DCA) is a potent inhibitor of pyruvate dehydrogenase kinase (PDK), resulting in the inhibition of lactate production, and has been shown to be effective in the treatment of patients with lactic acidosis [32]. DCA is also able to reduce muscle lactate accumulation in both animals and humans [33]. So, we reasoned that DCA may be able to attenuate SASM by decreasing lactate accumulation in muscles. To test this hypothesis, we first measured the effect of DCA on extracellular lactate levels in muscle cells. Supplementation of DCA eliminated the increased lactate production by fluvastatin (25% and 45% decrease compared to control and fluvastatin single treatment respectively), consisting with the potent glycolysis inhibitory activity of DCA (Fig. 6a). Next, DCA was co-administrated with lovastatin in mice for 30 days. The swimming endurance was significantly improved by DCA (Fig. 6b), in line with the recovered lactate levels in blood (Fig. 6c) and in GAS and TA muscles (Fig. 6d).

4. Discussion

Currently, the definition, epidemiology, diagnosis and management of SAMS are conflicting, which could be improved by further understanding of the pathophysiology of the symptoms. Several theories have been proposed, including sarcolemmal cholesterol reduction, isoprenoid depletion and mitochondrial dysfunction [34]. However, it has been demonstrated that nonstatin lipid-lowering agents fibrates induced myopathy through different pathways [35], which questions the sarcolemmal cholesterol reduction theory. As the target of RhoA, which is activated by prenylation, Akt phosphorylation is decreased with statin treatment [36]. But, our results with unchanged phosphor-Akt (Supplemental Fig. 3) and published data showing an increase with statin treatment [28] makes the isoprenoid depletion theory

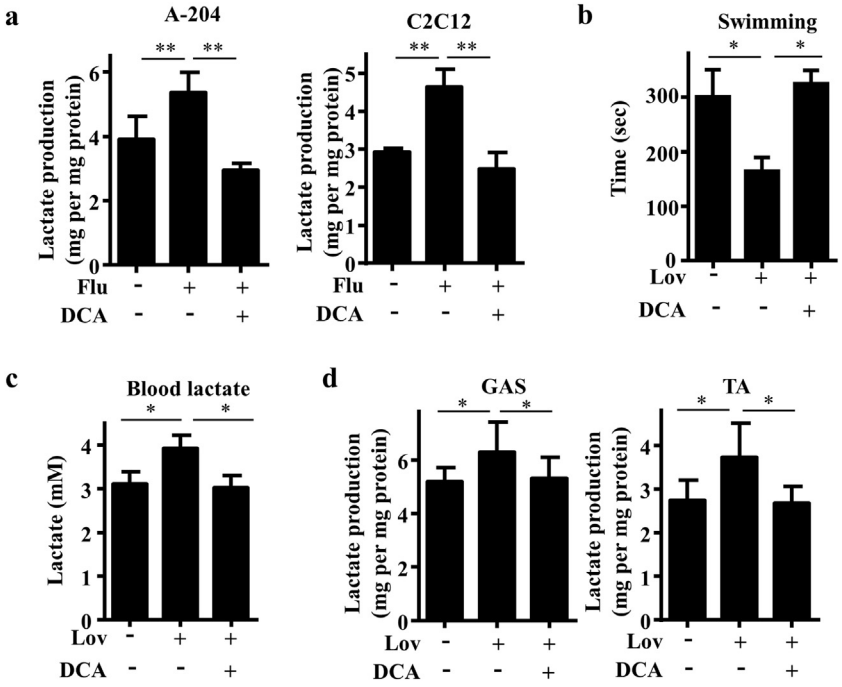

Fig. 6. Dichloroacetate antagonizes statin-induced lactate accumulation and improves mice exercise capacity. (a) Effect of dichloroacetate (DCA, 10 mM) on fluvastatin-induced lactate production in muscle cells (n = 3). (b) Maximum swimming duration times of C57BL/6 J mice co-administered with lovastatin and DCA for 30 days (*n* = 10 each group). (c) Resting blood lactate levels of C57BL/6 J mice co-administered with lovastatin and DCA for 30 days (n = 10 each group). (d) Lactate concentrations in gastrocnemius (GAS) and tibialis anterior (TA) muscles of C57BL/6 J mice co-administered with lovastatin and DCA for 30 days (n = 10 each group). Data are shown as mean ± SD, $^{*}P < .05$, $^{**}P < .01$ (one-way ANOVA, Tukey's test).

more complicated. Mitochondrial dysfunction is the most privileged hypotheses of SAMS. Nonetheless, it has been challenged [37–40], and supplementation of CoQ10 is inconclusive. Here, we provided another possibility that increased lactate, an important nociceptive substance in muscle complaints, may contribute to SAMS. It is supported by the fact that exercise exacerbates muscle syndromes induced by statins [41], as exercise will cause additional lactate accumulation. It is also consistent with previous findings that glycolytic muscles are more affected by statins [42]. At the meantime, we recognized the intricacy of the topic, with many studies showing little impact of statins on muscle symptoms [43], the lack of appropriate animal models [44], and studies showing no obvious elevation of lactate levels with statins treatment [16,17]. However, our findings represent a new insight into this field, and may be complementary to other hypotheses in different forms/contexts of SAMS. Together with the findings that statins inhibit monocarboxylate transporter 1 and 4 (MCT1 and MCT4) which are responsible for lactate uptake [36], our results do suggest clinical studies of the association of blood lactate levels with SAMS to be carried out.

Apart from the canonical tumor suppressive activities, the tumor suppressor p53 plays important roles in maintaining cellular health and function in skeletal muscle [45]. In this study, we found that statins decreased basal p53 levels through repressive regulation of β-enolase, resulting in compromised exercise capacity, which is consistent with previous findings in p53 knockout mice [46,47]. It has been reported that patients carrying inherited β-enolase deficiency present with a mild myopathy similar to some forms of SAMS [48,49]. The patients were glycolytic defective, which prevents energy production, similar to other inherited metabolic myopathies. While in our study, statin stimulated β-enolase promotes the nociceptive substance lactate production, resulting in muscle symptoms. Thus, it is possible that abnormal β-enolase promotes muscle symptoms at either insufficient or excessive levels under different mechanisms.

In this study, we showed that DCA reverted lactate elevation in blood and muscles and improved exercise capacity in mice treated with lovastatin, indicating its possible application against SAMS. In addition, DCA has been reported to increase mitochondrial oxidative metabolism leading to an improved cellular energy state in skeletal muscles [50], and revert simvastatin-induced CK elevation through inhibition of forkhead box protein O (FOXO) mediated proteolysis [51]. However, it is should be noted that other pharmacological effects of DCA, such as the non-competitive inhibitory effect on HMG-CoA reductase and induction of peripheral neuropathy, are potential confounding factors that may intervene in its use in SAMS [32]. Furthermore, DCA inhibits its own metabolism enzyme glutathione transferase zeta 1 (GSTZ1) in a chloride-dependent manner, resulting in delayed elimination upon repeated doses [32]. In the sarcoplasma, statins can affect the chloride channel conductance [36], raising another concern about drug interactions between statins and DCA. So caution should be taken in choosing the appropriate doses before the clinical trials of DCA on SAMS.

Acknowledgments

The SCO2 disrupted HCT116 cell line was a generous gift from Dr. Paul M. Hwang, NHLBI/NIH, USA.

Sources of funding

This work was supported by grants from the Science and Technology Development Fund (FDCT) of Macau to Ma (Project codes: 034/2015/A1 and 0013/2019/A1). The funder of the study had no role in study design, data collection, data analysis, data interpretation, or writing of the report. The corresponding author had full access to all the data in the study and had final responsibility for the decision to submit for publication.

Declaration of interests

The authors confirm that this article content has no conflicts of interest.

Author contributions

WM, LL and JH conceived this study, designed and performed experiments. WM, JH wrote and edited the manuscript. JD, WL, ZL, XH, NZ, YX performed the experiments and analyzed data.

Appendix A. Supplementary data

Supplementary data to this article can be found online at https://doi.org/10.1016/j.ebiom.2019.06.003.

References

[1] Weintraub WS. Perspective on trends in statin use. JAMA Cardiol 2017;2(1):11–2.
[2] Newman Connie B, Preiss D, Tobert Jonathan A, Jacobson Terry A, Page Robert L, Goldstein Larry B, et al. Statin safety and associated adverse events: a scientific statement from the American Heart Association. Arterioscler Thromb Vasc Biol 2019;39(2):e38–81.
[3] Serban MC, Colantonio LD, Manthripragada AD, Monda KL, Bittner VA, Banach M, et al. Statin intolerance and risk of coronary heart events and all-cause mortality following myocardial infarction. J Am Coll Cardiol 2017;69(11):1386–95.
[4] Backes JM, Ruisinger JF, Gibson CA, Moriarty PM. Statin-associated muscle symptoms-managing the highly intolerant. J Clin Lipidol 2017;11(1):24–33.
[5] Rosenson RS, Baker S, Banach M, Borow KM, Braun LT, Bruckert E, et al. Optimizing cholesterol treatment in patients with muscle complaints. J Am Coll Cardiol 2017;70(10):1290–301.
[6] Immke DC, McCleskey EW. Lactate enhances the acid-sensing Na+ channel on ischemia-sensing neurons. Nat Neurosci 2001;4(9):869–70.
[7] Salvemini D, Little JW, Doyle T, Neumann WL. Roles of reactive oxygen and nitrogen species in pain. Free Radic Biol Med 2011;51(5):951–66.
[8] Neale R, Reynolds TM, Saweirs W. Statin precipitated lactic acidosis? J Clin Pathol 2004;57(9):989–90.
[9] Goli AK, Goli SA, Byrd RP, Roy TM. Simvastatin-induced lactic acidosis: a rare adverse reaction? Clin Pharmacol Ther 2002;72(4):461–4.
[10] De Pinieux G, Chariot P, Ammi-Said M, Louarn F, Lejonc JL, Astier A, et al. Lipid-lowering drugs and mitochondrial function: effects of HMG-CoA reductase inhibitors on serum ubiquinone and blood lactate/pyruvate ratio. Br J Clin Pharmacol 1996;42(3):333–7.
[11] Limprasertkul A, Fisher NM, Awad AB, Pendergast DR. Statin therapy depresses fat metabolism in older individuals. J Am Coll Nutr 2012;31(1):32–8.
[12] Seachrist JL, Loi CM, Evans MG, Criswell KA, Rothwell CE. Roles of exercise and pharmacokinetics in cerivastatin-induced skeletal muscle toxicity. Toxicol Sci 2005;88(2):551–61.
[13] El-Ganainy SO, El-Mallah A, Abdallah D, Khattab MM, Mohy El-Din MM, El-Khatib AS. Rosuvastatin safety: an experimental study of myotoxic effects and mitochondrial alterations in rats. Toxicol Lett 2017;265:23–9.
[14] El-Ganainy SO, El-Mallah A, Abdallah D, Khattab MM, Mohy El-Din MM, El-Khatib AS. Elucidation of the mechanism of atorvastatin-induced myopathy in a rat model. Toxicology 2016;359-360:29–38.
[15] Song M, Chen FF, Yh Li, Zhang L, Wang F, Rr Qin, et al. Trimetazidine restores the positive adaptation to exercise training by mitigating statin-induced skeletal muscle injury. J Cachexia Sarcopenia Muscle 2018;9(1):106–18.
[16] Delliaux S, Steinberg JG, Lesavre N, Paganelli F, Oliver C, Jammes Y. Effect of long-term atorvastatin treatment on the electrophysiological and mechanical functions of muscle. Int J Clin Pharmacol Ther 2006;44(6):251–61.
[17] Galtier F, Mura T, Raynaud de Mauverger E, Chevassus H, Farret A, Gagnol JP, et al. Effect of a high dose of simvastatin on muscle mitochondrial metabolism and calcium signaling in healthy volunteers. Toxicol Appl Pharmacol 2012;263(3):281–6.
[18] Vaughan RA, Garcia-Smith R, Bisoffi M, Conn CA, Trujillo KA. Ubiquinol rescues simvastatin-suppression of mitochondrial content, function and metabolism: implications for statin-induced rhabdomyolysis. Eur J Pharmacol 2013;711(1–3):1–9.
[19] Piette AB, Dufresne SS, Frenette J. A short-term statin treatment changes the contractile properties of fast-twitch skeletal muscles. BMC Musculoskelet Disord 2016;17(1):449.
[20] Jung K, Kim IH, Han D. Effect of medicinal plant extracts on forced swimming capacity in mice. J Ethnopharmacol 2004;93(1):75–81.
[21] Godar S, Ince TA, Bell GW, Feldser D, Donaher JL, Bergh J, et al. Growth-inhibitory and tumor- suppressive functions of p53 depend on its repression of CD44 expression. Cell 2008;134(1):62–73.
[22] Muraki A, Miyashita K, Mitsuishi M, Tamaki M, Tanaka K, Itoh H. Coenzyme Q10 reverses mitochondrial dysfunction in atorvastatin-treated mice and increases exercise endurance. J Appl Physiol 2012;113(3):479–86.
[23] Bouitbir J, Charles AL, Rasseneur L, Dufour S, Piquard F, Geny B, et al. Atorvastatin treatment reduces exercise capacities in rats: involvement of mitochondrial impairments and oxidative stress. J Appl Physiol 2011;111(5):1477–83.

[24] Rosenson RS, Baker SK, Jacobson TA, Kopecky SL, Parker BA. The National Lipid Association's muscle safety expert P. An assessment by the statin muscle safety task force: 2014 update. J Clin Lipidol 2014;8(3):S58–71 Suppl.
[25] Apostolopoulou M, Corsini A, Roden M. The role of mitochondria in statin-induced myopathy. Eur J Clin Invest 2015;45(7):745–54.
[26] Sung HJ, Ma W, Wang PY, Hynes J, O'Riordan TC, Combs CA, et al. Mitochondrial respiration protects against oxygen-associated DNA damage. Nat Commun 2010;1:5.
[27] Ibi T, Sahashi K, Kato K, Takahashi A, Sobue I. Immunohistochemical demonstration of beta-enolase in human skeletal muscle. Muscle Nerve 1983;6(9):661–3.
[28] Morimoto Y, Bando YK, Shigeta T, Monji A, Murohara T. Atorvastatin prevents ischemic limb loss in type 2 diabetes: role of p53. J Atheroscler Thromb 2011;18(3):200–8.
[29] Kruiswijk F, Labuschagne CF, Vousden KH. p53 in survival, death and metabolic health: a lifeguard with a licence to kill. Nat Rev Mol Cell Biol 2015;16(7):393–405.
[30] Paajarvi G, Roudier E, Crisby M, Hogberg J, Stenius U. HMG-CoA reductase inhibitors, statins, induce phosphorylation of Mdm2 and attenuate the p53 response to DNA damage. FASEB J 2005;19(3):476–8.
[31] Johnson RA, Ince TA, Scotto KW. Transcriptional repression by p53 through direct binding to a novel DNA element. J Biol Chem 2001;276(29):27716–20.
[32] James MO, Jahn SC, Zhong G, Smeltz MG, Hu Z, Stacpoole PW. Therapeutic applications of dichloroacetate and the role of glutathione transferase zeta-1. Pharmacol Ther 2017;170:166–80.
[33] Hoshino D, Tamura Y, Masuda H, Matsunaga Y, Hatta H. Effects of decreased lactate accumulation after dichloroacetate administration on exercise training-induced mitochondrial adaptations in mouse skeletal muscle. Physiol Rep 2015;3(9).
[34] Abd TT, Jacobson TA. Statin-induced myopathy: a review and update. Expert Opin Drug Saf 2011;10(3):373–87.
[35] Joy TR, Hegele RA. Narrative review: statin-related myopathy. Ann Intern Med 2009;150(12):858–68.
[36] Souich PD, Roederer G, Dufour R. Myotoxicity of statins: mechanism of action. Pharmacol Ther 2017;175:1–16.
[37] Schaefer WH, Lawrence JW, Loughlin AF, Stoffregen DA, Mixson LA, Dean DC, et al. Evaluation of ubiquinone concentration and mitochondrial function relative to cerivastatin-induced skeletal myopathy in rats. Toxicol Appl Pharmacol 2004;194(1):10–23.
[38] Tay SK, Dimauro S, Pang AY, Lai PS, Yap HK. Myotoxicity of lipid-lowering agents in a teenager with MELAS mutation. Pediatr Neurol 2008;39(6):426–8.
[39] Hou T, Li Y, Chen W, Heffner RR, Vladutiu GD. Histopathologic and biochemical evidence for mitochondrial disease among 279 patients with severe statin myopathy. J Neuromuscul Dis 2017;4(1):77–87.
[40] Nakahara K, Kuriyama M, Sonoda Y, Yoshidome H, Nakagawa H, Fujiyama J, et al. Myopathy induced by HMG-CoA reductase inhibitors in rabbits: a pathological, electrophysiological, and biochemical study. Toxicol Appl Pharmacol 1998;152(1):99–106.
[41] Meador BM, Huey KA. Statin-associated myopathy and its exacerbation with exercise. Muscle Nerve 2010;42(4):469–79.
[42] Westwood FR, Scott RC, Marsden AM, Bigley A, Randall K. Rosuvastatin: characterization of induced myopathy in the rat. Toxicol Pathol 2008;36(2):345–52.
[43] Collins R, Reith C, Emberson J, Armitage J, Baigent C, Blackwell L, et al. Interpretation of the evidence for the efficacy and safety of statin therapy. Lancet (London, England) 2016;388(10059):2532–61.
[44] Stroes ES, Thompson PD, Corsini A, Vladutiu GD, Raal FJ, Ray KK, et al. Statin-associated muscle symptoms: impact on statin therapy-European atherosclerosis society consensus panel statement on assessment, Aetiology and management. Eur Heart J 2015;36(17):1012–22.
[45] Beyfuss K, Hood DA. A systematic review of p53 regulation of oxidative stress in skeletal muscle. Redox Rep 2018;23(1):100–17.
[46] Matoba S, Kang JG, Patino WD, Wragg A, Boehm M, Gavrilova O, et al. p53 regulates mitochondrial respiration. Science 2006;312(5780):1650–3.
[47] Park J-Y, Wang P-Y, Matsumoto T, Sung HJ, Ma W, Choi JW, et al. p53 improves aerobic exercise capacity and augments skeletal muscle mitochondrial DNA content. Circ Res 2009;105(7) [705-12, 11 p following 12].
[48] Comi GP, Fortunato F, Lucchiari S, Bordoni A, Prelle A, Jann S, et al. Beta-enolase deficiency, a new metabolic myopathy of distal glycolysis. Ann Neurol 2001;50(2):202–7.
[49] Musumeci O, Brady S, Rodolico C, Ciranni A, Montagnese F, Aguennouz M, et al. Recurrent rhabdomyolysis due to muscle beta-enolase deficiency: very rare or underestimated? J Neurol 2014;261(12):2424–8.
[50] Howlett RA, Heigenhauser GJF, Hultman E, Hollidge-Horvat MG, Spriet LL. Effects of dichloroacetate infusion on human skeletal muscle metabolism at the onset of exercise. Am J Physiol Endocrinol Metab 1999;277(1):E18–25.
[51] Mallinson JE, Constantin-Teodosiu D, Glaves PD, Martin EA, Davies WJ, Westwood FR, et al. Pharmacological activation of the pyruvate dehydrogenase complex reduces statin-mediated upregulation of FOXO gene targets and protects against statin myopathy in rodents. J Physiol 2012;590(24):6389–402.